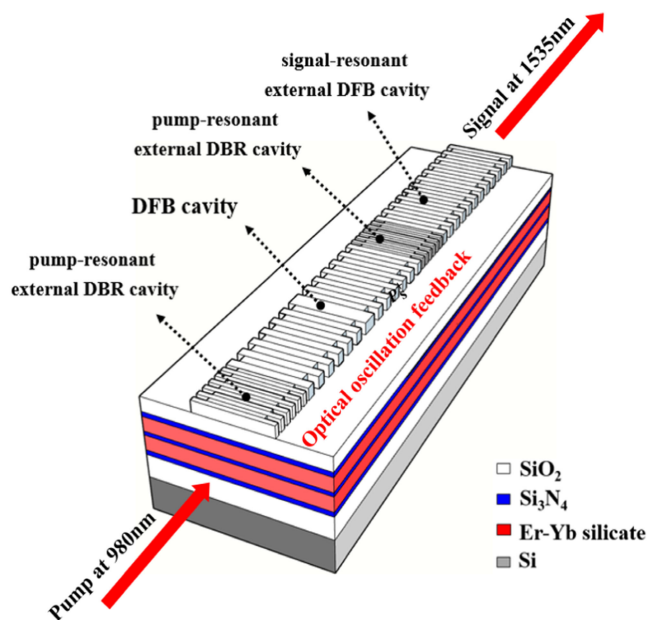# A Sub-kHz Narrow-Linewidth, and Hundred-mW High-Output-Power Silicon-Based Er Silicate Laser With Hybrid Pump and Signal Co-Resonant Cavity

Peiqi Zhou
Xingjun Wang
Yandong He

A Sub-kHz Narrow-Linewidth, and Hundred-mW High-Output-Power Silicon-Based Er Silicate Laser With Hybrid Pump and Signal Co-Resonant Cavity

Peiqi Zhou,[1,2,3] **Xingjun Wang** ,[1,3] **and Yandong He** [2]

[1]State Key Laboratory on Advanced Optical Communication Systems and Networks, School of Electronics Engineering and Computer Science, Department of Electronics, Peking University, Beijing 100871, China
[2]Institute of Microelectronics, School of Electronics Engineering and Computer Science, Peking University, Beijing 100871, China
[3]Frontiers Science Center for Nano-optoelectronics, Peking University, Beijing 100871, China

Abstract: Narrow-linewidth silicon-based lasersplay an important role in the field of silicon photonics. In this paper, we have proposed a high performance narrow-linewidth silicon-based Er silicate laser, based on strip-loaded DFB waveguide with a hybrid pump and signal co-resonant cavity. The saturated output power can reach over 90 mW at 1535 nm, with a maximum power conversion efficiency of 66%. The pump threshold is about 22 mW, and the laser linewidth is also as narrow as about 755 Hz. The results provide a new way for future scale integrated ultra-narrow-linewidth silicon-based lasers application.

Index Terms: Silicon photonics, DFB, waveguide laser.

1. Introduction

Silicon-based laser, as the critical part of silicon photonic devices, is one of the most attracting frontier topics in the field of silicon photonics. Especially, narrow-linewidth laser has great potential for high coherence, high frequency stability and wide wavelength tuning. Therefore, integration of high performance narrow-linewidth lasers on a silicon photonics platform is important for several applications, such as ultra-high-speed optical communication, long-distance space laser communication, ultra-high resolution Lidar, optical sensing and other fields [1]. In the traditional research, hybrid III-V silicon-based lasers usually integrate frequency-selective structures in resonators or couple with mode-selective devices outside resonators to control gain and loss at different wavelengths, so as to compress their laser linewidth [1]. They have been shown to generate several MHz optical linewidth with phase-shifted distributed feedback (DFB) cavities, but these approaches generally require complex fabrication steps, or careful temperature control [2]. Alternatively,

monolithic erbium (Er)-doped lasers have the advantages of temperature insensitivity, long luminescence lifetime, low noise and good compatibility with complementary metal-oxide-semiconductor (CMOS) technology [3]. They are more conducive to the large-scale integrated silicon-based lasers and shown to achieve kHz linewidths using a DFB cavity [4]. As Schawlow-Townes linewidth shows, higher laser output power, higher lasing efficiency, or higher quality factor (Q value) resonant cavities with low passive loss are required to further improve the linewidth. Accordingly, in 2013, Belt et $al.$ [5] demonstrated an array of integrated Al_2O_3:Er^{3+} waveguide-DFB lasers on an ultra-low-loss silicon nitride (Si_3N_4) planar waveguide platform. Lasing with output powers of 8 μW with a threshold of 81 mW are shown, and the FWHM lasing linewidth is about 501 kHz. Then, in 2016, Singh et $al.$ [6] designed a resonant pump cavity for the Er-doped DFB laser to recirculate the unabsorbed pump light and improve the narrow-linewidth lasing performance. The resonant cavity has higher quality factor, and they show an improvement of 1.8 times in the lasing efficiency when the DFB laser is pumped on-resonance, so the linewidth can be further reduced. In 2017, Purnawirman et $al.$ [7] designed distributed phase-shifted (DPS) cavities for Er-doped DFB lasers to achieve a several times improvement in laser output power. They obtained an ultra-narrow-linewidth laser output with maximum power of 5.43 mW (Pth = 14 mW). The slope efficiency was improved to 2.9%, and the optical linewidth was reduced to about 5.3 kHz.

However, current silicon-based lasers cannot achieve high quality narrow-linewidth laser output that can cater for the on-chip requirements in silicon photonics. On the one hand, the output power required by on-chip silicon-based lasers should be at least over 30 mW [3], and higher pump-to-laser efficiency is also needed to reduce the input pump power for the low power consumption demand. On the other hand, narrower laser linewidth, such as sub-kHz or Hz magnitude, is expected for future ultra-narrow-linewidth laser applications. Current narrow-linewidth lasers cannot meet those requirements. Therefore, two main technical schemes are proposed for solving these difficulties above. Firstly, the output power or efficiency improvement of the Er-doped lasers is limited by the gain limitation of Er-doped medium because of solid solubility. It is necessary to increase the Er^{3+} concentrations to further improve the gain property of the materials. Secondly, the original DFB cavity linewidth is severely confined by the length and loss factors of the resonator, so the cavity feedback is still at a low level. A more reasonable lasing resonator with higher Q value is required to optimize both pump absorption efficiency and signal optical feedback, which can not only greatly reduce the laser linewidth and threshold, but also improve the laser output power and efficiency.

In this paper, we have proposed a high performance silicon-based Er silicate laser, based on hybrid Er silicate-Si_3N_4 strip-loaded DFB waveguide with a pump and signal co-resonant cavity. Er silicate with high Er^{3+} concentration is used as active materials to further improve the lasing internal optical gain. And Er silicate-Si_3N_4 hybrid structure can help reduce the cavity loss. Then the high-performance laser outputs can be obtained by combining DFB resonator with a designed pump and signal co-resonant cavity. The maximum saturated output power can reach over 90 mW (the maximum power conversion efficiency is about 66%) at the lasing wavelength of 1535 nm with a pump threshold of 22 mW. And the laser linewidth can be as narrow as about 755 Hz. The results provide a new possibility for future scale integrated silicon-based lasers application.

2. Design and Modeling of Silicon-Based Er Silicate Laser With Pump and Signal Co-Resonant Cavity

Fig. 1 shows the structure diagram of the silicon-based Er silicate laser. As Fig. 1(a) shows, the laser structure is based on the hybrid Er silicate-Si_3N_4 strip-loaded DFB waveguide with pump and signal external co-resonant cavity, which has four features. Firstly, Er silicate has a high net gain attributable to its high Er concentration that has no insolubility problem. Such materials contain an high Er^{3+} concentration of $\sim 10^{22}$ cm^{-3} [8]–[12], which is two to three orders of magnitude higher than other Er-doped material ($\sim 10^{16}$ cm^{-3} to 10^{20} cm^{-3}) [3], [13]. In addition, ytterbium (Yb) cations are usually added into the Er silicate film to substitute Er^{3+} in the silicate lattice that can prevent
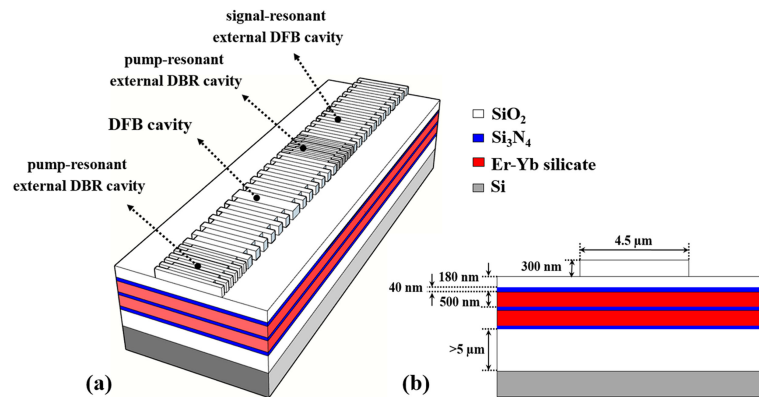
Fig. 1. Structure diagram of the silicon-based Er silicate laser. (a) 3-D design diagram of the laser structure. (b) Waveguide cross section and key parameter notes of the laser structure.
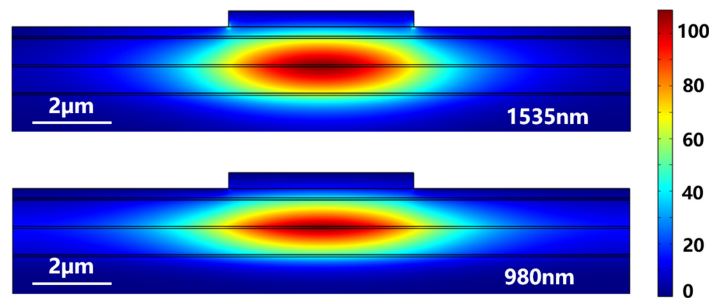

Fig. 2. The optical field distribution of the pumped light (980 nm) and the signal light (1535 nm) in the waveguide.

neighboring Er^{3+} from causing up-conversion, and they also act as sensitizers [11]. Such material results in the high gain of over 100 dB/cm, which can better improve the lasing output power and efficiency. Secondly, the hybrid Er silicate-Si_3N_4 alternate stack is used to reduce the loss of waveguide effectively, because of the low optical loss characteristics of Si_3N_4 itself [14]. Thirdly, the strip-loaded structure solves the etching problem for Er silicate laser resonators. The SiO_2 spacer is added to ensure single-mode transmission of the signal and to control the propagation confinement factor more effectively. The maximum allowed waveguide size has been chosen for single-mode transmission with good energy confinement and convenient light input coupling. Fourthly, a DFB micro-cavity is designed to obtain main optical feedback for 1535 nm signal, which is the key to lasing. This laser wavelength is chosen corresponding to the strongest photoluminescence peak of Er silicate thin film [15]. Two 980 nm pump DBR cavities are added on the either side of main DFB cavity to improve pump absorption efficiency. Then a 1535 nm external signal DFB cavity is appended on the end side of the cavity to provide additional optical feedback. Such a hybrid resonant cavity with high quality factor can greatly improve the laser performance, such as laser output power, efficiency, linewidth and threshold.

The waveguide cross section of the laser structure is shown in Fig. 1(b). Key parameters of the waveguide structure design, such as the thickness of Er silicate film and Si_3N_4 sub-layer, the size of strip-loaded waveguide, and the thickness of SiO_2 spacer, are optimized to improve the confinement factor in gain layer and the overlapping intensity of pump light (980 nm) and signal light (1535 nm). The optical field distributions of the pumped light (980 nm) and the signal light (1535 nm) in the waveguide simulated by COMSOL are shown in Fig. 2. It can be seen that the signal and pump mode are both chosen for single-mode transmission with good confinement in the waveguide. And the confinement factors of the pumped light and the signal light in the gain region are calculated as 95% and 91%, respectively.
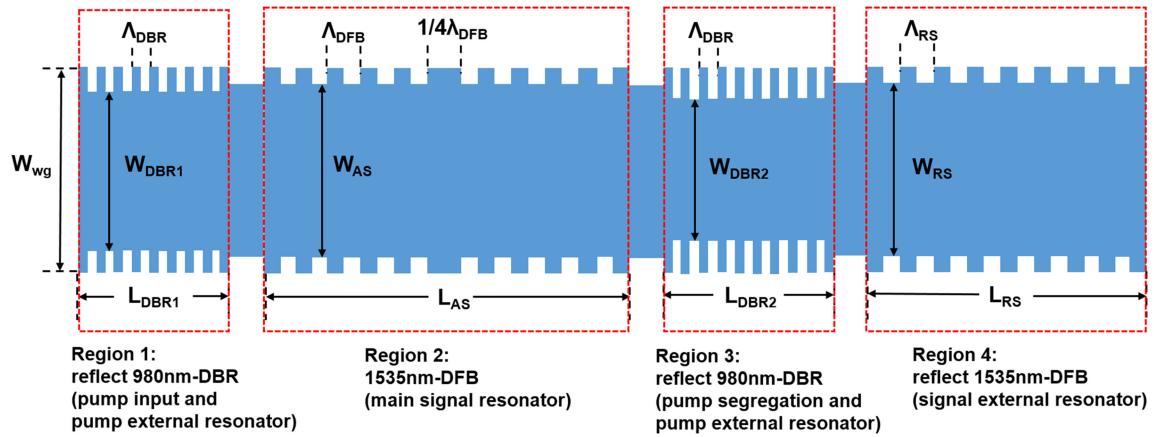
Fig. 3. Structure of hybrid DFB resonator with pump and signal external co-resonant cavity. This hybrid resonator can be further refined into four regions. Region 2 is a basic DFB resonator that provides main optical feedback for lasing. Region 1 and 3 act as two 980 nm DBR reflectors, which provide additional pump feedback. Region 4 plays the role of 1535 nm DFB resonator at the end of the cavity, which provides additional signal feedback.

Fig. 3 shows the structure of hybrid DFB resonator with pump and signal co-resonant external cavity. Such pump and signal co-resonant external cavity can be divided into two parts, the 980 nm pump external resonant cavity that helps improving pump absorption efficiency, and 1535 nm signal external resonant cavity that helps enhancing signal resonance intensity. Furthermore, this hybrid resonator can be further refined into four regions, that have different actions and design processes. Accordingly, region 2 is a basic DFB resonator that provides main optical feedback for lasing. Region 1 and 3 act as two 980 nm DBR reflectors, which provide additional pump feedback. Region 4 plays the role of 1535 nm DFB reflector at the end of cavity, which provides additional signal feedback. Detailed design processes for these four regions are discussed following.

Region 1 is a 980 nm DBR resonator, which acts as pump injection and pump external reflector at left-end of main resonator. The central wavelength of the resonator is set as 980 nm by designing the grating period, Λ, following the Bragg condition as:

$$\Lambda = \frac{\lambda}{2n_{eff}},$$ (1)

where n_{eff} is the effective refractive index corresponding to the cross section of waveguide. In this cross section, the hybrid Er silicate-Si_3N_4 stack and strip-loaded waveguide are taken as a whole to calculate this effective refractive index, which can obtain the grating more accurately. The reflectivity of the DBR grating should be set as a reasonable value, which ensures enough pump input and left-end pump reflection at the same time. It is designed with the duty cycle (D) and tooth depth of the grating, determined by the reflectivity (R) calculation as follows:

$$R = tanh(\kappa L),$$ (2)

where L is the cavity length, κ is the grating coupling coefficient, that can be calculated as [14]:

$$\kappa = \frac{\Gamma \left(n_h^2 - n_l^2 \right)}{\lambda n_{eff}} sin(\pi D)),$$ (3)

where n_h and n_l are the high and low refractive index of the grating, which depend on the grating tooth depth. Γ represents the confinement factor in the grating waveguide region at the central wavelengths.

Region 2 is a 1535 nm DFB resonator, which acts as main signal resonator that provides main optical feedback for lasing. The grating parameters, like period, duty cycle and tooth depth, are

following original optimized DFB parameters. These values are designed to decide the grating strength that can ensure the resonator can provide enough optical feedback and generate a maximum laser output power. The single-longitudinal-mode operation for Er silicate waveguide laser is typically possible for cavities with suitable κL values, which corresponds to DFB grating tooth depth of 0.65 μm. Also, the length of this main DFB cavity should be set in a reasonable range of 4.5–6.5 mm. The shorter cavity has weak optical feedback and low gain, resulting in low laser output power. But when cavity length become too longer, the gain media will completely absorbed the pump in the waveguide. Here too, the remainder of the waveguide was not pumped but absorbed the signal while there was no population inversion. This leads to insufficient pumping distance. In addition, a 1/4 phase shift region is introduced into the DFB cavity in order to suppress the phase shift during signal transmission that can ensure the stable output of single mode laser.

Region 3 is a 980 nm DBR resonator, which acts as pump segregating region and pump external reflector at right-end of main resonator. The reflectivity of this DBR region should be set at near 100%, because it is designed in combination with the length of region 4 to ensure that the pump is completely segregated by region 3 and does not enter the 1535 nm reflect region. This point will make the 1535 nm DFB grating provide pure signal feedback without unnecessary gain in region 4. After calculating by Eq. (2) and (3), the tooth depth should be set as more than 0.8 μm, while the DBR resonator length is set as 200 μm (100% reflectivity for 980 nm pump, and 100% transmissivity for 1535 nm signal).

The two DBR resonators of region 1 and 3 form a pump external resonant cavity together. Pump feedback is provided in this region to form 980 nm pump resonance in the cavity and improve its absorption efficiency. It is necessary to control the Q value of this DBR external cavity, in order to ensure that the resonance loss of 980 nm pump in external cavity is less than that of in internal cavity. As the parameters of DBR grating in region 3 are determined, the DBR grating design in region 1 is based on matching the external Q value to internal Q value of DFB cavity, for critical coupling [6]. The external Q value of DBR external cavity is calculated using the following formula [6]:

$$Q = \frac{2\pi \nu_0}{\log\left(\frac{1}{R_1 R_2}\right) \frac{\upsilon_p}{2L}}, \tag{4}$$

where ν_0 is the resonance frequency, υ_p is the phase velocity. R_1 and R_2 are the DBR grating reflectivity on left and right sides. And the internal Q is calculated to be $(1.4–1.9)\times10^4$, corresponding to different cavity length, 4.56.5 mm. Fig. 4 shows the matching graph of the external Q and internal Q at different cavity lengths. The Q value of DBR external cavity increases with the increase of DBR grating tooth depth. This is because deeper teeth have greater optical feedback, resulting in larger reflectivity. The Q value matching points are the intersections of dotted lines (internal Q at different cavity length) and black curve (external Q) in Fig. 4. Thus the DBR tooth depth of region 1 can be set as about 0.40 μm, 0.42 μm, 0.44 μm, 0.46 μm, and 0.48 μm for internal DFB lengths under 4.5 mm, 5 mm, 5.5 mm, 6 mm, and 6.5 mm, respectively. Finally, the left-end reflectivity for 980 nm pump feedback and input is calculated as a range of 80%–90% while the DBR external cavity length is set as 140 μm, as shown in the triangular lines.

Region 4 is a 1535 nm DFB resonator, which acts as a signal sub-resonator for lasing. When the pump power is segregated completely by region 3, there is no unnecessary pump absorption in region 4, so this kind of external DFB reflector can offer a pure signal reflection. As a result, it provides additional feedback with well-controlled phase to the laser, which makes the whole cavity generate external signal resonance, so the laser output power and conversion efficiency are further improved while the pump threshold is reduced. The grating size of this external DFB reflector is the same as main DFB resonator, which prevents 1535 nm signal light from producing phase difference. And the cavity length of this external DFB reflector is designed by optimizing its reflectivity, that aims at ensuring enough 1535 nm optical feedback. Fig. 5 shows the output power of the Er silicate waveguide laser with designed pump resonant DBR cavity as a function of signal external DFB reflectivity at different pump power. The curves show that the laser output power first
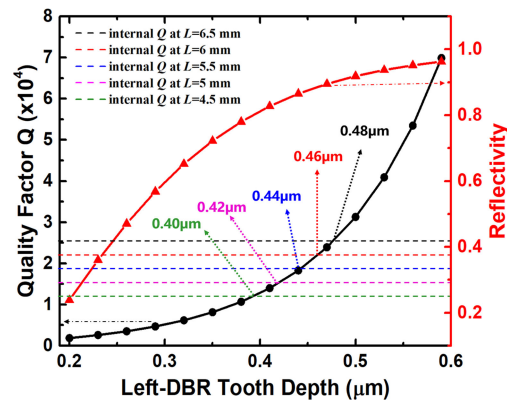
Fig. 4. The DBR external Q versus DBR grating tooth depth (circular line) and reflectivity versus DBR grating tooth depth (triangular line). The Q value matching points are the intersections of dotted lines (internal Q at different cavity length) and the curve, corresponding to the left-DBR tooth depth of about 0.40 μm, 0.42 μm, 0.44 μm, 0.46 μm, and 0.48 μm for internal DFB lengths under 4.5 mm, 5 mm, 5.5 mm, 6 mm, and 6.5 mm, respectively. Finally, the left-end reflectivity for 980 nm pump feedback and input is calculated as a range of 80%–90% while the DBR external cavity length is set as 140 μm, as shown in the triangular lines.
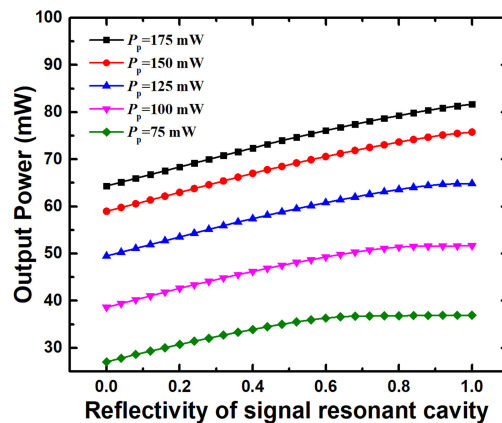

Fig. 5. Output power of the Er silicate waveguide laser with pump resonant DBR cavity as a function of signal external DFB reflectivity at different pump power (75–175 mW). The main cavity length is fixed at 5.5 mm.

increases linearly with signal external DFB reflectivity, but as the reflectivity continues to increase, the power increases slowly or even saturates. It suggests that the laser output power increases with increase in reflectivity of the signal external DFB cavity, because of larger lasing feedback. Then, the increase of laser power further enhances Er^{3+} stimulated radiation in the active region. Thus, this effect causes the Er^{3+} concentration in the excited state to reduce more rapidly, more pump power is needed to form population inversion. The given pump power is completely absorbed in main cavity, resulting in laser power saturation. And this saturation becomes deeper with the increasing of input pump power. Therefore, the external DFB cavity length of region 4 should be chosen as reasonable values, larger than 5 μm, for different input pump power.

In summary, the structure parameters of the optimized Er silicate-Si_3N_4 mixed film strip-loaded waveguide laser and the hybrid pump and signal co-resonant cavity are shown in Table 1.

The signal operation in this hybrid DFB waveguide cavity can be divided into two sections, the active section and reflect section. And it is described mathematically by coupled-mode theory. The signal power is split into the forward and backward propagating modes in the DFB regions.

TABLE 1

Structure Parameters of the Optimized Er Silicate-Si_3N_4 Mixed Film Strip-Loaded Waveguide Laser

Parameters	Symbol	Values
Parameters of Waveguide Sturcture		
SiO_2 substrate thickness	t_{oxide}	>5 μm
Si_3N_4 sublayer thickness	$t_{nitride}$	40 nm
Er silicate layer thickness	t_{Er}	500 nm
strip-loaded waveguide thickness	$t_{strip-loaded}$	300 nm
strip-loaded waveguide width	$W_{strip-loaded}$	4.5 μm
strip-loaded waveguide width	$W_{strip-loaded}$	4.5 μm
Parameters of Region 1		
DBR grating period	Λ_{DBR}	470 nm
DBR grating duty ratio	D	50%
DFB grating tooth depth	gtd_{DBR1}	0.4~0.48 μm
Region 1 length	L_{DBR1}	200 μm
Parameters of Region 2		
DFB grating period	Λ_{DBR}	470 nm
DFB grating duty ratio	D	50%
DFB grating tooth depth	gtd_{DFB}	0.65 μm
DFB 1/4 phase shift region length	$L_{1/4\lambda}$	470 nm
Region 2 length	L_{AS}	4.5~6.5 mm
Parameters of Region 3		
DFB grating tooth depth	gtd_{DBR2}	>0.8 μm
Region 3 length	L_{DBR2}	200 μm
Parameters of Region 4		
DFB grating period	Λ_{RS}	470 nm
DFB grating tooth depth	gtd_{RS}	0.65 μm
Region 4 length	L_{RS}	>500 μm

In the case of a uniform Bragg grating, the signal coupling between the two counter-propagating modes with gain effect is described by the following set of coupled-mode equations [16]–[19] (set the cavity left-end to z = 0):

$$
\begin{cases}
\frac{dA(z)}{dz} = \begin{cases} -j\kappa B(z)exp(j2\Delta\beta z - j\theta) + \frac{g_s(z)}{2}A(z), & L_{DBR_1} < z < L_{DBR_1} + L_{AS} \\ -j\kappa B(z)exp(j2\Delta\beta z), & L_{DBR_1} + L_{AS} + L_{DBR_2} < z < L_{DBR_1} + L_{AS} + L_{DBR_2} + L_{RS} \end{cases} \\
\frac{dB(z)}{dz} = \begin{cases} -j\kappa A(z)exp(j2\Delta\beta z + j\theta) - \frac{g_s(z)}{2}B(z), & L_{DBR_1} < z < L_{DBR_1} + L_{AS} \\ -j\kappa A(z)exp(j2\Delta\beta), & L_{DBR_1} + L_{AS} + L_{DBR_2} < z < L_{DBR_1} + L_{AS} + L_{DBR_2} + L_{RS} \end{cases}
\end{cases} , \quad (5)
$$

where $A(z)$ and $B(z)$ are the amplitudes of the forward and backward propagating modes, respectively. j is the imaginary unit. θ is the phase shift in the DFB grating transmission, which can be set as 0 and π before and after the 1/4 phase shift region, respectively. $\Delta\beta$ is a measure of the deviation from the Bragg condition. And the $g_s(z)$ is the net gain coefficient of Er silicate for signal light per unit length.

The pump operation in this hybrid DFB waveguide cavity is described mathematically by propagation equations. And the two DBR gratings are rather considered as effective reflectors. Those equations are also given in two directions because of the co-propagation and contra-propagation

TABLE 2

Parameters of Modeling Er-Yb Silicate Compound in the Preceding Calculations and Analysis

Parameters	Values	References
Er^{3+} concentration	$3.3 \times 10^{21} cm^{-3}$	[15]
Yb^{3+} concentration	$1.7 \times 10^{22} cm^{-3}$	[15]
Er^{3+} emission cross section at 1532 nm	$1.24 \times 10^{-20} cm^{-3}$	[11], [20], [21]
Er^{3+} absorption cross section at 1532 nm	$1.24 \times 10^{-20} cm^{-3}$	[11], [20], [21]
Er^{3+} emission cross section at 980 nm	$2.58 \times 10^{-21} cm^{-3}$	[11], [20], [21]
Yb^{3+} emission cross section at 980 nm	$1.2 \times 10^{-20} cm^{-3}$	[11], [20], [21]
Yb^{3+} absorption cross section at 980 nm	$1.2 \times 10^{-20} cm^{-3}$	[11], [20], [21]
Er^{3+} emission lifetime at $^4I_{13/2}$ level	7.8 ms	[20], [22]
cooperative upconversion coefficient of Er^{3+}	$5 \times 10^{-17} cm^3/s$	[20], [22]
Er^{3+} cross-relaxation coefficient	$3.5 \times 10^{-17} cm^3/s$	[20], [22]
Yb^{3+}-to-Er^{3+} energy-transfer coefficient	$2.26 \times 10^{-16} cm^3/s$	[20], [22]
propagation loss of Er silicate	3 dB/cm	[14]
propagation loss of Si_3N_4	0.1 dB/cm	[7]

for pump in the resonator. So the pumping transmission equations are expressed as follows:

$$\frac{dP_p^{\pm}(z)}{dz} = \mp g_p(z)P_p^{\pm}(z), \qquad (6)$$

where the $g_p(z)$ is the net absorption coefficient of Er silicate for pump light per unit length. The gain and absorption coefficient of signal and pump can be expressed by the steady-state rate equations, using the multi-energy levels model of Er-Yb silicate system [20]. And the corresponding parameters of Er silicate thin film are extracted according to previous study of $Er_xYb_{2-x}SiO_5$ thin films [15], [21]. Table 2 summarizes the parameters used for modeling Er-Yb silicate compound in the preceding calculations and analysis.

The final laser output power is proportional to the sum of $|A(z)|^2$ and $|B(z)|^2$, which can be describe as:

$$P_s(z) = \frac{2\varepsilon_0 n_{eff}^2}{h\nu_s}\left(|A(z)|^2 + |B(z)|^2\right), \qquad (7)$$

where ν_s is the signal frequency.

The hybrid cavity laser acts as a self-sustained oscillator where the entire lasing is generated inside the main DFB cavity. The assumed boundary conditions are given in the sense that there is no incident laser field, as follows:

$$\begin{cases} P_p^+(L_{DBR_1}) = R_{DBR_1} \cdot P_p^-(L_{DBR_1}) + (1 - R_{DBR_1}) \cdot P_{input\,pump} \\ P_p^-(L_{DBR_1} + L_{AS}) = R_{DBR_2} \cdot P_p^+(L_{DBR_1} + L_{AS}) \\ P_s^+(L_{DBR_1}) = 0 \\ P_s^{\pm}(L_{DBR_1} + L_{AS} + L_{DBR_2}) = \mp \alpha L_{DBR_2} + P_s^{\pm}(L_{DBR_1} + L_{AS}) \\ P_s^-(L_{DBR_1} + L_{AS} + L_{DBR_2}) = R_{RS} \cdot P_s^{\pm}(L_{DBR_1} + L_{AS} + L_{DBR_2}) \\ P_{laser\,output} = P_s^-(L_{DBR_1}) - \alpha L_{DBR_1} \end{cases} \qquad (8)$$

3. Results and Discussion

Fig. 6 shows the output power of the Er silicate strip-loaded DFB waveguide laser without resonant external cavity as a function of cavity length at different pump power. A threshold gain for optical
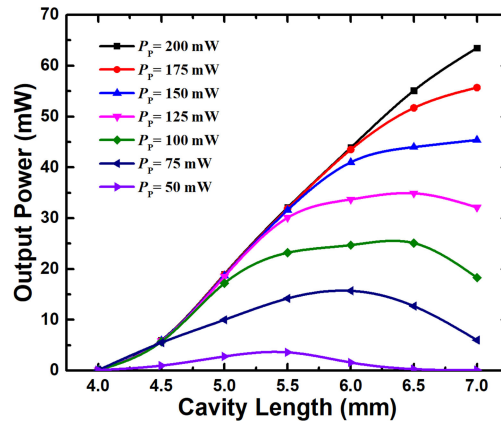
Fig. 6. Output power versus cavity length (07 mm) with different pump power (50–200 mW) of the Er silicate strip-loaded DFB waveguide laser without external resonant cavity.
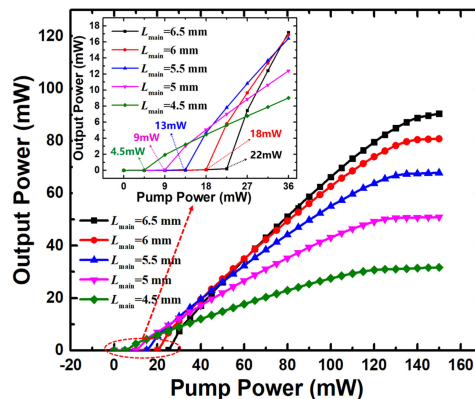

Fig. 7. Output power of the optimized cavity versus pump power (0–200 mW) with different cavity length (4.5–6.5 mm). The inset shows an expanded view of the red-dashed region for pump powers 0–36 mW. The threshold pump power reached approximately 4.5 mW, 9 mW, 13 mW, 18 mW, and 22 mW for resonator lengths under 4.5 mm, 5 mm, 5.5 mm, 6 mm, and 6.5 mm, respectively.

resonators exists to ensure the photon steady-state oscillation condition, and this will correspond to a threshold cavity length. It can be seen that the threshold resonator length is about 4 mm. And the laser output power increases with increase of cavity length and then tends to satuate or even decrease. The short cavity has weak optical feedback and low gain, resulting in low laser output. And the long length of resonant cavity leads to insufficient pumping distance, the remainder of the cavity was not pumped but, rather, absorbed the signal while there was no population inversion. Therefore, the length of the cavity should be set in a reasonable range of 4.56.5 mm. As a result, the output power can reach near 23 mW for 5.5 mm cavity length with pump power of 100 mW without improvement of external resonantor.

Fig. 7 shows the output power of Er silicate strip-loaded DFB waveguide laser with designed external resonant cavity as a function of pump power at different cavity length. It can be seen that the laser output power increases with increases in pump power and gradually saturates. This result occurs because increases in signal power further enhance Er^{3+} stimulated radiation, thus causing more rapid reductions in the Er^{3+} concentration of the excited state. This reduction, in turn, restrains the further amplification of the signal, resulting in laser output saturation that slows as the cavity length increases. The laser output performance has been improved under the action of the designed external resonant cavity. The output power can reach near 65 mW for 5.5 mm cavity
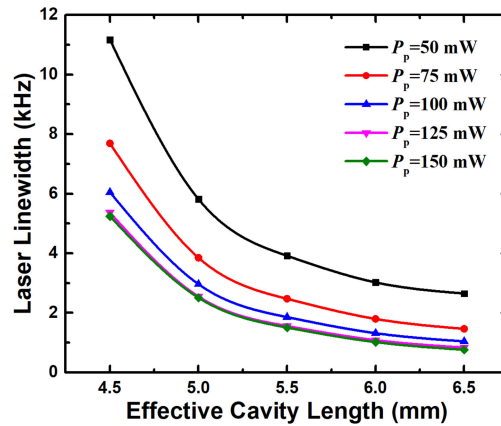
Fig. 8. Laser linewidth versus effective cavity length (4.56.5 mm) with different pump power (50–150 mW).

length with pump power of 100 mW, which is about 2.5 times higher than the DFB waveguide laser without external resonant cavity. And the maximum saturated output power can reach over 90 mW with the increase of cavity length and pump power. The device also shows high pump-to-laser power conversion efficiency. According to the calculation of Fig. 7, the power conversion efficiency is about 27.5%, 43.1%, 55.1%, 62.6%, and 66.3% for main DFB resonator lengths under 4.5 mm, 5 mm, 5.5 mm, 6 mm, and 6.5 mm, respectively. The maximum power conversion efficiency is as high as near 66%. Such high output power with high power conversion efficiency can satisfy the power requirement for on-chip silicon-based lasers, which is mentioned above. Moreover, the threshold pump power also decreases due to the enhancement of pumping efficiency. As the inset to Fig. 7 shows, the threshold pump power is approximately from 4.5 mW to 22 mW for main DFB resonator lengths under 4.5 mm to 6.5 mm, respectively. Generally, these results indicate that those high-power and low-threshold silicon-based waveguide lasers can better cater for the output power requirement and low power consumption demand in future on-chip laser application.

In addition, this DFB resonator with hybrid pump and signal co-resonant cavity presents a strong resonance intensity that leads to a narrow laser linewidth. The linewidth of the single-mode laser can be expressed as the full half-peak width (FWHM) of the optical emission spectrum, which is limited by the spontaneous emission in the DFB cavity. The laser linewidth can be theoretically calculated by modified Schawlow-Townes formula, which accounts for possible intrinsic cavity losses as well as reabsorption losses, as follows [23], [24]:

$$\Delta v_L = \frac{2\pi h v_L (\Delta v_c)^2}{P_{laser\,output}} \left[1 - \frac{\tau_p}{\tau_{loss}}\right] \left[1 - \frac{\sigma_{abs}(c\tau_p\sigma_{em}N_{Er} - 1)}{\sigma_{em}(c\tau_p\sigma_{abs}N_{Er} + 1)}\right]^{-1}, \tag{9}$$

where Δv_c is the passive cavity linewidth, τ_p and τ_{loss} are the photon and loss decay time, σ_{abs} and σ_{em} are the effective absorption and emission cross-sections at 1535 nm, and N_{Er} is the Er^{3+} concentration in Er silicate. Fig. 8 shows the calculated laser linewidth as a function of effective cavity length at different pump power. The linewidth of laser output decreases with the increase in effective cavity length and gradually paces down. This is because the passive cavity linewidth changes with the cavity length. The cavity linewidth is expressed in terms of the photon lifetime as [17]:

$$\Delta v_c = \frac{1}{2\pi\tau_p} = \frac{P}{2\pi E_c} = \frac{P_{laser\,output}}{2\pi E_c} + \frac{P_{loss}}{2\pi E_c} = \frac{2v_{eff}}{2\pi \Gamma L_{eff}} + \frac{\alpha_{loss}v_{eff}}{2\pi} = \frac{v_{eff}}{2\pi}\left(\frac{2}{\Gamma L_{eff}} + \alpha_{loss}\right), \tag{10}$$

where E_c denotes the energy stored in the cavity, v_{eff} is the effective group velocity, and α_{loss} is the internal cavity loss. Γ is the confinement factor, given by the ratio of the average signal intensity inside the cavity to the average signal intensity from both facets. The increase in effective cavity
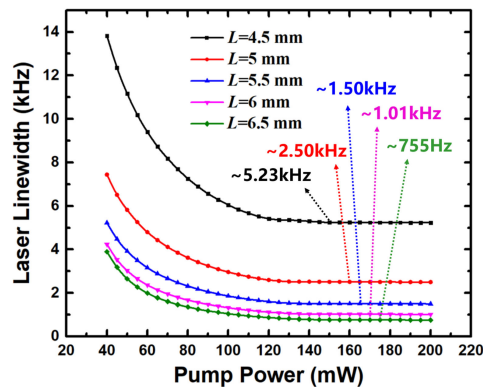
Fig. 9. Laser linewidth versus pump power (40200 mW) with different cavity length (4.56.5 mm). The limit laser linewidth reached approximately 5.23 kHz, 2.50 kHz, 1.50 kHz, 1.01 kHz, and 932 Hz and 755 Hz for effective DFB resonator lengths under 4.5 mm, 5 mm, 5.5 mm, 6 mm, and 6.5 mm, respectively.

length results in the decrease in passive cavity linewidth, also as the increase in output power. Therefore, the laser linewidth becomes narrower. And such downward trend gradually weakens because of the laser output saturation, as shown in Fig. 6. The laser linewidth and cavity length of this configuration, considered together, are competitive: longer-size lasers can be used to improve the laser linewidth, while smaller-size lasers can be used to reduce the input pump power and meet the scale integration requirement.

The laser linewidth also decreases with the increase of the pump power. Fig. 9 shows the calculated laser linewidth as a function of pump power at different cavity length. The linewidth of laser output decreases with the increase in pump power and gradually tends to a limit value. As the pump power increases, the laser output power increases and consequently the number of stimulated emitted photons in the cavity, each spontaneous emitted photon which is coupled to the laser mode will have a less pronounced effect on the perturbation of the laser emission, so the laser linewidth becomes narrower. Then the linewidth tends to a limit value while the output power saturates with the pump power, as shown in Fig. 7. It can be seen from Fig. 9 that the limit laser linewidth reached approximately 5.23 kHz, 2.50 kHz, 1.50 kHz, 1.01 kHz, and 932 Hz and 755 Hz for effective DFB resonator lengths under 4.5 mm, 5 mm, 5.5 mm, 6 mm, and 6.5 mm, respectively. Above all, such a sub-kHz narrow-linewidth, hundred-mW high-power silicon-based Er silicate laser better caters for the future on-chip narrow-linewidth laser application requirements.

For feasibility, this proposed device design can be achieved experimentally by the similar processes to those experimental device of Al_2O_3:Er^{3+} DFB laser [5], [7]. Substrate functionalization, stacking of hybrid Er silicate-Si_3N_4 layers, and fabrication of strip-loaded waveguide DFB resonators are compatible with CMOS current processes.

4. Conclusion

In summary, we have demonstrated a silicon-based Er silicate laser that based on hybrid Er silicate-Si_3N_4 strip-loaded DFB waveguide with a pump and signal co-resonant cavity. Both pump absorption efficiency and signal optical feedback are optimized in this hybrid cavity and the laser presents high-performance lasing outputs. A sub-kHz narrow-linewidth of 755 Hz was obtained for the laser with co-resonant cavity. The laser output power can reach over 90 mW with a high power conversion efficiency of 66% after designing external resonant cavity, which is about 2.5 times higher than traditional DFB waveguide lasers. The pump threshold is also as low as about 22 mW. The results indicate this Er silicate waveguide laser with high performance as potential candidate that can better cater for the on-chip laser requirements, and such device will provide a new way for future scale integrated narrow-linewidth silicon-based lasers application.

References

[1] Y. N. Du, C. Chen, L. Qin, Y. Y. Chen, and Y. Q. Ning, "Narrow linewidth external cavity semiconductor laser based on silicon photonic chip," *Chin. Opt.*, vol. 12, no. 2, pp. 230–240, 2019.

[2] B. R. Koch *et al.*, "Narrow linewidth external cavity semiconductor laser based on silicon photonic chip," *Laser Photon. Rev.*, vol. 3, no. 4, pp. 355–369, 2009.

[3] J. D. B. Bradley and M. Pollnau, "Erbium-doped integrated waveguide amplifiers and lasers," *Laser Photon. Rev.*, vol. 5, no. 3, pp. 368–403, 2011.

[4] E. H. Bernhardi *et al.*, "Ultra-narrow-linewidth, single-frequency distributed feedback waveguide laser in Al_2O_3:Er^{3+} on silicon," *Opt. Lett.*, vol. 5, no. 3, pp. 368–403, 2010.

[5] M. Belt, T. Huffman, M. L. Davenport, W. Li, J. S. Barton, and D. J. Blumenthal, "Arrayed narrow linewidth erbium-doped waveguide-distributed feedback lasers on an ultra-low-loss silicon-nitride platform," *Opt. Lett.*, vol. 38, no. 22, pp. 4825–4 828, 2013.

[6] G. Singh *et al.*, "Resonant pumped erbium-doped waveguide lasers using distributed Bragg reflector cavities," *Opt. Lett.*, vol. 41, no. 6, pp. 1189–1192, 2016.

[7] P. Purnawirman *et al.*, "Ultra-narrow-linewidth Al_2O_3:Er^{3+} lasers with a wavelength-insensitive waveguide design on a wafer-scale silicon nitride platform," *Opt. Exp.*, vol. 25, no. 12, pp. 13 705–13 713, 2017.

[8] H. Isshiki, M. J. A. D. Dood, A. Polman, and T. Kimura, "Self-assembled infrared-luminescent Er-Si-O crystallites on silicon," *Appl. Phys. Lett.*, vol. 85, no. 19, pp. 4343–4345, 2004.

[9] M. Miritello *et al.*, "Efficient luminescence and energy transfer in erbium silicate thin films," *Adv. Mater.*, vol. 19, no. 12, pp. 1582–1588, 2007.

[10] X. J. Wang, G. Yuan, H. Isshiki, T. Kimura, and Z. Zhou, "Photoluminescence enhancement and high gain amplification of $er_xy_{2-x}sio_5$ waveguide," *J. Appl. Phys.*, vol. 108, no. 1, 2010, Art. no. 013506.

[11] X. J. Wang *et al.*, "Extraordinary infrared photoluminescence efficiency of $Er_0.1Yb_{1.9}SiO_5$ films on Sio_2/Si substrates," *Appl. Phys. Lett.*, vol. 98, no. 7, 2011, Art. no. 079103.

[12] X. J. Wang, L. J. Jiang, R. M. Guo, R. Ye, and Z. P. Zhou, "Spontaneous emission rate and optical amplification of Er^{3+} in double slot waveguide," *Sci. China Phys., Mech. Astron.*, vol. 58, no. 12, pp. 124 201–124 201, 2015.

[13] Y. H. Wang, C. S. Ma, D. L. Li, and D. M. Zhang, "Gain characteristics of Er^{3+}/Yb^{3+} co-doped waveguide amplifiers," *J. Semicond.*, vol. 29, no. 3, pp. 578–582, 2008.

[14] L. Wang, R. M. Guo, B. Wang, X. J. Wang, and Z. P. Zhou, "Hybrid Si_3N_4-Er/Yb silicate waveguides for amplifier application," *IEEE Photon. Technol. Lett.*, vol. 24, no. 11, pp. 900–902, 2012.

[15] P. Q. Zhou, X. J. Wang, Y. D. He, Z. F. Wu, J. L. Du, and E. G. Fu, "Effect of deposition mechanisms on the infrared photoluminescence of erbium-ytterbium silicate films under different sputtering methods," *J. Appl. Phys.*, vol. 125, 2019, Art. no. 175114.

[16] C. L. Chen, *Foundations for Guided wWave Optics*. New York, NY, USA: Wiley, 2007.

[17] K. Kikuchi and H. Tomofuji, "Analysis of oscillation characteristics of separated-electrode DFB laser diodes," *IEEE J. Quantum Electron.*, vol. 26, no. 10, pp. 1717–1727, Oct. 1990.

[18] M. Yamada and K. Sakuda, "Analysis of almost-periodic distributed feedback slab waveguides via a fundamental matrix approach," *Appl. Opt.*, vol. 26, pp. 3474–3478, 1987.

[19] M. A. Rodriguez, M. S. Malcuit, and J. J. Butler, "Transmission properties of refractive index-shifted Bragg gratings," *Opt. Commun.*, vol. 177, pp. 251–257, 2000.

[20] P. Q. Zhou *et al.*, "High-gain erbium silicate waveguide amplifier and a low-threshold, high-efficiency laser," *Opt. Exp.*, vol. 26, no. 13, pp. 16 689–16 707, 2018.

[21] X. J. Wang, P. Q. Zhou, Y. D. He, and Z. P. Zhou, "High-gain erbium silicate waveguide amplifier and a low-threshold, high-efficiency laser," *Opt. Mater. Express*, vol. 8, no. 10, pp. 2970–2990, 2018.

[22] A. Shooshtari, T. Touam, and S. I. Najafi, "Yb^{3+} sensitized Er^{3+}-doped waveguide amplifiers: A theoretical approach," *Opt. Quantum Electron.*, vol. 30, no. 4, pp. 249–264, 1998.

[23] H. Haken, "Laser theory," in *Encyclopedia of Physics*, vol. XXV 2C. New York, NY, USA: Springer, 1970.

[24] A. L. Schawlow and C. H. Townes, "Infrared and optical masers," *Phys. Rev.*, vol. 112, 1958, Art. no. 1940.